F-10-06 Extended Abstracts of the 2020 International Conference on Solid State Devices and Materials, VIRTUAL conference, 2020, pp407-408

Non-Destructive 9.35GHz Microwave Sensing System for Investigating Electrical Properties of Silicon

Toshiyuki Sameshima[1], Masahiko Hasumi[1], and Tomohisa Mizuno[2]

[1] Tokyo University of Agriculture and Technology
2-24-16 Naka-cho, Koganei, Tokyo 184-8858, Japan
Phone: +81-42-388-7109 E-mail: tsamesim@cc.tuat.ac.jp
[2] Kanagawa University
Hiratsuka, Kanagawa 259-1293, Japan

Abstract

Non-destructive two-dimensional monitoring in semiconductor processing is reported with 9.35 GHz microwave transmittance system. Changes in the sheet resistivity R_s and photo-induced minority carrier lifetime τ_{eff} were successfully monitored in the process steps of thermal oxidation, ion implantation, and heat treatment for pn junction formation. Moreover, change in τ_{eff} with bias voltage applied to the pn junction is experimentally analyzed with the present sensing method.

1. Introduction

Non-destructive monitoring of electrical properties is important for semiconductor device processing [1]. For example, the resistivity and effective minority carrier lifetime τ_{eff} can change during the fabrication steps. We have developed non-destructive 9.35 GHz microwave sensing system for detecting the majority and minority carriers in semiconductor [2,3]. In this paper, we report a measurement method to precisely measure two-dimensional distribution of the sheet resistivity R_s and τ_{eff} of crystalline silicon substrates at the process steps of thermal oxidation, ion implantation, and its activation to form the pn junctions. Moreover, we demonstrate change in τ_{eff} of the samples with pn junctions with bias voltages application under 450, 635 and 980 nm light illumination [4].

2. Experimental

Figure 1(a) shows a schematic microwave transmittance measurement system for non-destructively measuring electrical properties of semiconductors. 9.35 GHz microwave was introduced with waveguide tubes, which had a narrow gap for placing a sample. The X-Y moving stage moved the sample to measure two-dimensional spatial distribution of electrical properties. The continuous wave (CW) 450, 635 and 980 nm laser diode (LD) lights were introduced in the waveguide tube to generate photo-induced carriers. They have different optical penetration depths in crystalline silicon as 0.26, 2.7 and 120 μm, respectively [5]. The light intensities at the sample surface were set at 2.1, 1.5 and 0.98 mW/cm^2, respectively, to realize the same photon flux among the different wavelength lights. Microwave transmittances in dark field T_d and under light illumination T_p were measured using a high-speed detector. Moreover, the system is constructed under bias voltage application to the sample to investigate properties of built-in potential in semiconductor as shown in Fig. 1(b). Al electrodes were conformal formed at the top and bottom surfaces of the sample. The light shade limited the illumination area to 2 mm from the electrode. T_d and T_p were measured coincidently with different bias. We constructed a finite element numerical calculation program to analyze the experimental data. The free carrier microwave absorption effect and the optical interference effect using a Fresnel coefficient are included in the calculation of the transmissivity [2,6]. Physics of photo-induced carrier generation, diffusion, and annihilation are also used for obtaining R_s and τ_{eff} [7].

13 Ωcm n-type single crystalline silicon substrates with a thickness of 500 μm and a crystalline orientation of (100) coated with 100 nm thick thermal grown SiO_2 layer were prepared. The ion implantation of boron and phosphorus atoms with concentrations of 1.0×10^{15} cm^{-2} were conducted at 25 and 75 keV for the top and bottom surfaces, respectively. The sample was subsequently heated at 900^{o}C for 5 min in air by the heating equipment with carbon heating tube [8]. After removing SiO_2 layer, Al electrodes were formed.

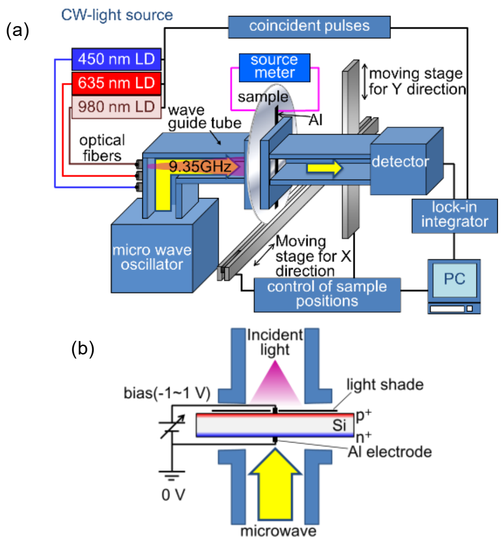

Fig. 1 (a) Schematic 9.35 GHz microwave transmittance measurement system and (b) cross sectional image of transmittance measurement under bias voltage application to the sample.

3. Results and Discussion

Figure 2 shows distribution of R_s and τ_{eff} of samples (a) as-grown with SiO_2 layers, (b) as-implanted, and (c) 900^{o}C-heated. There was distribution of R_s probably because of distribution of dopant atoms in the substrate as shown in Fig.

2(a). τ_{eff} was large ranging from 1.2 to 1.8 ms because good surface passivation was realized by thermal grown SiO_2. The density of recombination defects at the surfaces was estimated from 6.7×10^9 to 1.0×10^{10} cm^{-2} [9]. Ion implantation hardly changed the distribution of R_s as shown in Fig. 2(b). However, τ_{eff} markedly decreased from 2 to 10 μs by the implantation. 900°C heating effectively decreased R_s from 45 to 62 Ω/sq as shown in Fig 2(c). The dopant atoms were effectively activated, and the carrier density par unit area was estimated from 1.9×10^{15} to 1.3×10^{15} cm^{-2} if the carrier mobility was assumed as 60 cm^2/Vs in doped silicon. τ_{eff} markedly increased from 110 to 170 μs over the whole area by 900°C heating. Recombination defect density was estimated from 1.1×10^{11} to 1.6×10^{11} cm^{-2}. Dopant activation and defect reduction were simultaneously achieved by heating.

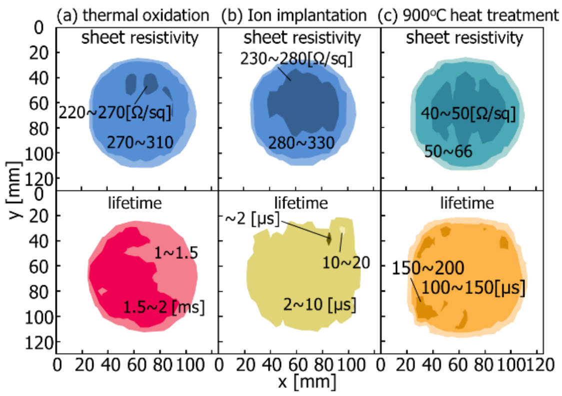

Fig. 2 Distribution of R_s and τ_{eff} of the samples (a) as-grown with SiO_2 layers, (b) as-implanted, and (c) 900°C-heated.

Figure 3 shows (a) current density in the dark and under the 635 nm light illumination at 1.2 mW/cm^2 and (b) τ_{eff} for the 450, 635 and 980 nm light illumination as a function of bias voltage. A typical diode rectified characteristic and photovoltaic effect were observed as shown in Fig. 3(a). The p+n junction was successfully formed by 900°C heating. τ_{eff} for the 450 nm light ranged from 6.5×10^{-6} to 7.7×10^{-6} s for the bias voltage lower than 0.2 V as shown in Fig. 3(b). It markedly increased to 1.2×10^{-4} s as the bias voltage increased to 0.5 V and then, it levelled off. Similar and slightly high τ_{eff} was obtained for the 635 nm light. However, the change in τ_{eff} for the 980 nm light was small compared with the other cases. τ_{eff} ranged from 1.3×10^{-4} to 1.5×10^{-4} s for the bias voltage lower than 0.3 V. It slightly increased to 1.8×10^{-4} s at 0.5 V and then, it also levelled off. These results indicate that penetration depth of the incident light is important for the change in τ_{eff} with bias voltage. Low τ_{eff} at low bias conditions indicates that the photo-induced minority (hole) carriers do not tend to move to the n-type silicon bulk. This is probably because the high built-in potential caused by low bias blocks the diffusion of minority carriers. Especially, 450-nm light illumination generate photo-induced carriers mainly in the p+ region according to the short penetration depth of 0.26 μm. In contrast, the built-in potential decreases by the high positive bias application. It allows the diffusion of hole carriers into the bulk region. The minority carrier density and τ_{eff} consequently increase for the high positive bias. 980 nm light illumination generate the photo-induced carriers in the band flat region of silicon bulk even in the negative bias condition because of the long penetration depth. The photo-induced carriers diffuse over the bulk region and τ_{eff} becomes high.

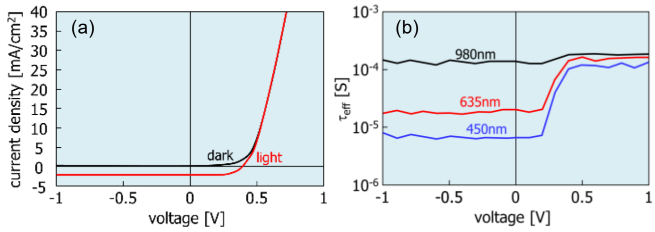

Fig. 3 (a) Current density in the dark field and under the 635 nm light illumination at 1.2 mW/cm^2 and (b) τ_{eff} for the 450, 635 and 980 nm light illumination as a function of bias voltage.

4. Conclusions

This paper demonstrated the two-dimensional distribution of R_s and τ_{eff} of the crystalline silicon substrates at the steps of thermal oxidation of surfaces, ion implantation, and its activation to form the pn junctions using the non-destructive 9.35 GHz microwave monitoring system. Decrease in R_s from 45 to 62 Ω/sq was successfully observed by the ion implantation followed by 900°C heating. Defect passivation was also observed by the transmittance monitoring with light illumination. We also demonstrated change in τ_{eff} of the silicon samples with pn junctions under bias voltages application. Low τ_{eff} was observed in the case of low bias application under 450 and 635 nm light illumination probably because the high built-in potential protected the diffusion of photo-induced hole carriers into the n-type silicon bulk region.

Acknowledgements

This work was partially supported by Japan Science and Technology Agency ASTEP (No. AS3015022S) and a Grants-in-Aid for Scientific Research C (No. 18K04225) from the Ministry of Education, Culture, Sports, Science and Technology of Japan.

References

[1] S. M. Sze: *Semiconductor Devices,* Wiley, New York, (1985).
[2] T. Sameshima, H. Hayasaka, T. Haba, J. Appl. Phys. **48** (2009) 021204.
[3] T. Sameshima, J. Furukawa, T. Nakamura, S. Shigeno, T. Node, S. Yoshidomi, M. Hasumi, Jpn. J. Appl. Phys. **53** (2014) 031301.
[4] T. Sameshima, T. Motoki, K. Yasuda, T. Nakamura, M. Hasumi, T. Mizuno, Jpn. J. Appl. Phys. **54** (2015) 081302.
[5] E. D. Palk, *Handbook of Optical Constants of Solids*, Academic Press, London (1985) pp. 562-577.
[6] M. Born and E. Wolf, *Principles of Optics, 6th ed.*, Cambridge, Cambridge University Press (1980).
[7] A.S. Groove, *Physics and Technology of Semiconductor Devices*, Willey, New York (1967) Chapter 5.
[8] T. Sameshima, T. Miyazaki, G. Kobayashi, T. Arima, T. Kikuchi, T. Uehara, T. Sugawara, M. Hasumi, I. Serizawa, IEEE Access **7** (2019) 23798.
[9] D. J. Fitzgerald and A. S. Grove, IEEE **54** (1966) 1601.